CHAPTER IV

SIGNIFICANT ENHANCEMENT OF THERMAL STABILITY IN THE NON-OXIDATIVE THERMAL DEGRADATION OF BISPHENOL-A/ANILINE BASED POLYBENZOXAZINE AEROGELS

4.1 Abstract

Previously we reported synthesis of a new type of organic aerogel from phenolic resins called polybenzoxazines and their transformation into carbon aerogels. Here, we further investigate the thermal degradation behaviors of both bulk polybenzoxazines and polybenzoxazine aerogels. It was found that the polybenzoxazine aerogels exhibit much greater degradation temperatures and char yields than the bulk. The decomposition temperature at 10% weight loss and the char yield at 800 °C of the bisphenol-A/aniline based polybenzoxazine aerogel increased up to 24% and 97% higher, respectively, than the corresponding values of the bulk. Kinetic investigation indicated that the bulk polybenzoxazine exhibits three stages of decomposition reaction, whereas the polybenzoxazine aerogel features four stages with a much higher overall activation energy for the decomposition reaction. Thermal degradation behaviors of the bulk polybenzoxazine and the polybenzoxazine aerogel were studied using Fourier transform infrared spectroscopy (FTIR), thermal gravimetric analysis (TGA)/FTIR, and gas chromatography (GC)/time of flight-mass spectroscopy (TOF-MS). The activation energy (Ea) of the decomposition step was determined using the Kissinger method.

(Key-word: Benzoxazine; Benzoxazine aerogel; Thermal degradation; Kinetics; Char yield)

4.2. Introduction

Aerogels are porous materials which consist of many contiguous micropores. Aerogel morphology can be modified using different synthesis parameters, a characteristic which makes aerogel particularly well adapted for various applications, such as in fuel cells, as host material for catalysts, thermal insulators, and molecular sieves [1]. Among various types of aerogel, carbon aerogels are of particular interest for applications as electrodes for supercapacitors, advanced catalyst supports, chromatographic packing, and adsorbents [2, 3]. Commonly, the physical process leading to carbon aerogel involves carbonization of an organic aerogel at high temperatures (600–900°C) under an inert atmosphere [1, 3-5]. With increasing interest in the study of carbon aerogel derived from polymeric substrates, the thermal decomposition of polymeric precursors has been widely investigated. Many previous researches reveal that the characteristic properties of residual char depend on various pyrolysis parameters, e.g. feedstocks, temperature, pressure, heating-cooling rate and soaking time [6, 7].

As new polymeric precursors for carbon aerogel, polybenzoxazines are a recently developed class of phenolic resins. Generally, polybenzoxazines are synthesized via a thermal ring-opening polymerization of aromatic oxazine compounds [8-10]. They provide many advantageous characteristics compared with traditional phenolic resins, such as high thermal stability and excellent mechanical properties, easy processibility, low water absorption, near zero shrinkage after polymerization, and excellent molecular design flexibility [11-13]. In previous studies, we have shown that bisphenol-A/aniline based polybenzoxazine organic aerogel and its related carbon aerogel can be successfully prepared via the sol-gel process [1]. The results indicate that the chemical structure of the obtained polybenzoxazine aerogel is essentially identical to the corresponding bulk polybenzoxazine. Since their chemical structures are similar, it is expected that their decomposition behaviors should also be very similar. Surprisingly, however, we found that their thermal decomposition behaviors are significantly different. The polybenzoxazine aerogel exhibited a much higher degradation temperature and char yield than the bulk polybenzoxazine. As mentioned earlier, while many

carbonization factors are known to affect the decomposition reaction and the properties of residual char, morphological differences are rarely observed between bulk polymer and aerogel. Following these interesting earlier results, a detailed investigation of the decomposition process of both bulk polybenzoxazine and polybenzoxazine aerogel was performed and is presented here.

Although many studies [14-17] have explored the thermal decomposition and solid state thermal degradation mechanism and kinetics of many types of polybenzoxazines, the influence of the physical structure of polybenzoxazine aerogel on the decomposition mechanism and the decomposition products has not yet been elucidated. The bulk polybenzoxazine and the polybenzoxazine aerogel used in this study are based on bisphenol-A and aniline. The thermal decomposition mechanisms of these two distinct polybenzoxazine morphologies were compared in detail. The residual chars at various sintering temperatures, and the volatile products evolved during the thermal decomposition processes of both bulk polybenzoxazine and polybenzoxazine aerogel were analyzed using scanning electron microscopy (SEM), Fourier transform infrared spectroscopy (FTIR), Thermogravimetric Analysis (TGA) coupled to FTIR (TGA-FTIR), Gas chromatography (GS) coupled to time-of-flight mass spectroscopy (GC-TOF-MS). Moreover, the activation energies (E_a) of their degradation reactions were also determined by the Kissinger method.

4.3 Experimental

4.3.1 Reaction Kinetic Theory

A change in slope and the occurrence of a peak in differential thermal analysis (DTA) represent changes in the thermal properties of a sample material associated with thermal reaction. When the reaction rate varies with temperature, the activation energy of the reaction can be calculated from the variation in position of the highest reaction rate with the heating rate, when the other experimental conditions are fixed [18]. For a simple decomposition reaction, the decomposition rate can be calculated from the mass consumption during the reaction, described by a basic rate equation, as follows:

$$\frac{d\alpha}{dt} = kf(\alpha)$$

where

$$\alpha = \frac{w_0 - w_t}{w_0 - w_\infty}$$

where w_t is the weight of a sample at time t, w_0 is the initial weight, and w_∞ is the final weight of a sample. According to the Arrhenius equation, the dependence of the reaction rate constant (k) of a decomposition reaction on temperature and activation energy is described by:

$$k = Ae^{-Ea/RT}$$

where A is a constant, Ea is the apparent activation energy, R is the gas constant, and T is absolute temperature.

According to extensive prior work, f(α) depends on the decomposition reaction mechanism [17, 19]. For the direct calculation of the activation energy from these equations, the decomposition reaction mechanism has to be known. Kissinger [18] proposed a mathematical model to enable calculation of the activation energy of solid state thermal reactions without any knowledge of the reaction mechanism (eq. 1). Using this method, the activation energy of a reaction can be obtained from the relationship between the applied heating rate in an experiment and the position of the highest reaction rate at each heating rate. The relevant equation is:

$$\ln\left(\frac{\beta}{T_P^2}\right) = \ln\frac{AR}{E_a} + \ln[n(1-\alpha_P)^{n-1}] - \frac{E_a}{RT_P} \qquad (1)$$

where n is the apparent reaction order, T_p is the absolute temperature at which the maximum weight-loss rate occurs, α_p is the fraction of decomposition at maximum weight-loss rate, and β is the heating rate in the experiment

Based on the Kissinger model, when $\ln(\beta/T_P^2)$ is plotted against $1/T_P$, a straight line is obtained with slope equal to $-E_a/R$, yielding an estimate of the apparent activation energy (E_a).

4.3.2 Materials

The materials used in this research are benzoxazine resin and xylene as solvent. The benzoxazine resin was based on bisphenol-A, aniline, and formaldehyde. Bisphenol-A (97%) and para-formaldehyde (95%) were purchased

from Sigma-Aldrich Company. Aniline (99%) was purchased from Panreac Quimica SA Company, and the solvent, xylene (98%), was obtained from Carlo Erba Reagenti.

4.3.3 Polybenzoxazine and Polybenzoxazine Aerogel Preparation

The benzoxazine monomer was synthesized via the solventless process proposed by Ishida [20]. Bisphenol A, aniline, and paraformaldehyde at a 1:2:4 molar ratio were mixed together and heated at 110 °C for 60 min until the mixture became a transparent pale yellow color. The monomer was used without further purification. The fully cured bulk polybenzoxazine was obtained by the step-heating of the acquired monomer at 160, 180 °C for an hour at each temperature and 200 °C for 2 h [1]. Then, the specimen was finally left to cool to room temperature before further characterization.

According to the aerogel synthesis method proposed by [1], benzoxazine solution was prepared from a benzoxazine monomer using xylene as a solvent. The monomer concentration was kept at 40 wt%. The mixture was transferred into vials and sealed. The temperature was slowly raised to 130 °C for 96 h. The attained product was a partially-cured benzoxazine hydrogel. The organic aerogel was then obtained by drying the hydrogel at ambient temperature and pressure for 2 days before step-heating to obtain fully cured organic aerogel, using the same heating process as the bulk polymerization.

4.3.4 Characterization of Polybenzoxazine and Polybenzoxazine Aerogel

SEM imaging of the microstructure of the bulk polybenzoxazine and the polybenzoxazine aerogel was performed on a HITACHI TM-1000 microscope at an acceleration voltage of 10 kV. The sample was adhered to a carbon sticky tape and coated with gold before the microstructure image of the sample was taken. TGA and differential TGA (DTG) analysis of generated volatile decomposition products was performed using a TGA Q50 with coupled to a Thermo Nicolet Nexus 670 FT-IR analyzer. The examinations were performed over a temperature range of 100 to 900 °C under a nitrogen flow of 90 mL/min, using a sample size of 20–30 mg. Furthermore, GC-TOF-MS was also used to identify the resulting volatile products.

The volatile decomposition products from TGA/DTG were dissolved in 20 mL of 1,4 dioxane, and the resulting solution was subjected to GC-TOF-MS analysis (GC7890A, Agilent Technologies, Palo Alto, CA, USA, and PEGASUS 4D TOF-MS, LECO Instrument GmbH, Monchengladbach, Germany) using Rtx-5 (RESTEK) 10m x 0.18mm x 0.20μm and Rtx-17 (RESTEK) 1.1m x 0.10mm x 0.10μm columns. The injection port of the GC was set at 250 °C. The GC temperature program was started at 70 °C and maintained for 1 min before raising the temperature to 250 °C with a heating rate of 5 °C/min. The Rtx-5 and Rtx-17 separation units used in this study were 5% and 50% phenylemethyl siloxane coated capillary columns, respectively. For chemical compound identification, mass spectrogram matching was performed using NIST MS search 2.0 library searching software.

FTIR spectra of the residual chars of the bulk polybenzoxazine and the polybenzoxazine aerogel at various sintering temperatures were obtained on a Thermo Nicolet Nexus 670 FT-IR analyzer at a resolution of 4 cm^{-1}. The sample was ground, mixed with KBr powder, and pressed into a pellet.

For kinetic analyses of the samples after obtaining their TGA/DTG thermograms, the Kissinger model was applied to the overlapping peaks within the thermograms. To separate the peaks of the DTG thermogram, nonlinear curve fitting was achieved using Peak fit program with controlling R^2 larger than 0.995. Moreover, linear curve fitting in the Kissinger model was obtained using Kaleida Graph 3.6 software. In this analysis, the TGA experiments were performed with heating rates of 10, 15, and 20 °C/min.

4.4 Results and Discussion

From our previous study [1], a new type of organic aerogel was successfully prepared from a new class of phenolic resins called polybenzoxazine, and converted into carbon aerogel via pyrolysis under inert atmosphere. During the study, we observed distinct differences in physical structures and char yields between the residual chars derived from the bulk polybenzoxazine and the polybenzoxazine aerogel. Figure 4.1 shows photography of cubic samples of the bulk polybenzoxazine and the polybenzoxazine aerogel, together with their residual chars after TGA

analysis, carried out over a temperature range from room temperature to 900 °C, at a heating of 15 °C/min.

As seen in the figure, the residual char of the bulk polybenzoxazine exhibits a swollen non-uniform foam-like structure underneath a glittering skin layer. The shape of the obtained char has changed from a cube to round. As expected for a typical foaming process, gases generated during decomposition of the bulk polybenzoxazine have inflated the polybenzoxazine into a swollen foam-like structure. In contrast, the shape of the residual char derived from the polybenzoxazine aerogel did not significantly change from its original shape and its volume has contracted slightly. This distinct behavior can be related to their different microstructures, shown in Figure 4.2, which compares SEM micrographs at 1000x magnification for the bulk polybenzoxazine and polybenzoxazine aerogel. The polybenzoxazine aerogel exhibits a very fine uniform porous structure with pore sizes of single digit micrometer length scale. In addition, the enlargement shown within the figure reveals a continuous polymer network incorporated with contiguous open pores analogous to previous studies [1, 5]. Thus, the generated gases are able to pass through these many open pores without any pressure created within the structure of the aerogel during the carbonization process, maintaining the physical structure.

Much to our surprise, we observed that not only the shape of their residual chars, but also their residual weights were significantly different. Figure 4.3 reveals TG and DTG thermograms of the bulk polybenzoxazine and the polybenzoxazine aerogel under nitrogen atmosphere at a heating of 15 °C/min. Each sample begins to decompose into volatile material around 240 °C, as indicated by the initial decrease of their retention weights. This observed onset decomposition temperature is in line with many other related works [1, 14, 15, 17]. Also in agreement with earlier work, the apparent weight loss of the bulk polybenzoxazine predominantly occurred in the temperature range between 300 and 500 °C. The degradation rate slowed dramatically above 500 °C and significant mass loss could not be observed beyond 800 °C. In addition, the degradation temperature at 10% weight loss and the char yield at 800 °C of the bulk polybenzoxazine were determined to be 342 °C and 27 wt%, respectively. Furthermore, according to DTG peak resolution displayed in

Figure 4.4a, the DTG thermogram of the bulk polybenzoxazine exhibits a three-stage decomposition process, which is also consistent with earlier studies [15, 17].

Since the chemical structures of bulk and aerogel were found to be similar [1], it was expected that their decomposition behaviors would be very close to each other. Interestingly, however, the polybenzoxazine aerogel exhibited significantly higher degradation temperature and char yield than the bulk. As observed in Figure 4.3, the decomposition temperatures at 5% weight loss and the char value at 800 °C of the aerogel were 369 °C and 51wt%, respectively. In addition, from TGA curve fitting shown in Figure 4.4b, the polybenzoxazine aerogel exhibits a four-stage decomposition process. To gain insight into these interesting TGA results, the influence of morphology change on the decomposition process of polybenzoxazine was further investigated. Figure 4.5 shows the FTIR spectra of the benzoxazine monomer, the bulk polybenzoxazine, and the polybenzoxazine aerogel. The characteristic absorption bands of benzoxazine monomer appear at 1240 and 1035 cm^{-1} (symmetric stretching of C–O–C), and 950 and 1500 cm^{-1} (tri-substituted benzene ring) [21]. Compared with the spectra of polybenzoxazine, the absorption bands in these regions disappear after the step cure, as seen in Figure 4.5b and c. These results are strongly in agreement with the study of Takeichi [22], suggesting that the peak disappearance is due to the ring-opening polymerization of the benzoxazine monomer. According to the ring-opening mechanism, a tetra-substituted benzene ring and hydrogen-bonded hydroxyl group are generated with absorption bands of 1460–1480 cm^{-1} and 1620 cm^{-1}, respectively [22, 23]. Upon detailed comparison between the absorption bands of the bulk polybenzoxazine and the polybenzoxazine aerogel, a additional absorption intensity around 1650 cm^{-1} characteristic of the C=N group can be observed for the aerogel. Also, the absorption band at 1200 cm^{-1}, corresponding to the C-N-C asymmetric deformation, is distinctly weaker in the case of aerogel. This evidence is consistent with the formation of a small amount of Schiff base during the polybenzoxazine aerogel synthesis. Based on the aerogel synthesis procedure, pregelled polybenzoxazine must be kept at high temperature for 96 h, which likely causes chain cleavage at the Mannich bridge (-CH_2-NR-CH_2-) within the polybenzoxazine chain to form the Schiff base end group. In many researches, the Schiff base has been considered as a defect structure, or a

terminal group of benzoxazine polymerization reaction, or the outcome of thermal decomposition, as shown in Scheme 4.1 [14, 15, 24].

The residual char of both the bulk polybenzoxazine and the polybenzoxazine aerogel at various sintering temperatures were examined by FTIR, as shown in Figure 4.6. Evidently, the residual chars obtained from both types of polybenzoxazine reveal similar typical FTIR characteristic absorption peaks, i.e. 750 cm^{-1} (mono-substituted benzene ring), 1200 cm^{-1} (C-N-C asymmetric deformation), 1460–1480 (tetra-substituted benzene ring), and 1550–1600 (C=C unsaturated aromatics, C=N unsaturated heterocycle) [22, 23, 25, 26]. Similarly seen in both figures, a decrease in the intensity of all organic absorption peaks was clearly observed, when the sintering temperature was increased from 400 to 800 °C. Upon close inspection, the intensity decrease in the polybenzoxazine aerogel is seen to be slower than that of the bulk. This is most clearly manifested as the presence of more intense organic FTIR absorption signal in the residual char derived from the polybenzoxazine aerogel at 600 °C, compared to that of the bulk at the same temperature. Specifically, at sintering temperatures higher than 600 °C, two asymmetric broad absorption bands extending from 1000 to 1600 cm^{-1} can be observed. It can be seen in Figure 4.6 that the two bands from the residual char obtained from the polybenzoxazine aerogel have more intensity than those from the bulk. These bands are generally known to reflect the coalescence of the vibrational modes of C=N, C–N, and C=C bonds [27-29]. Nevertheless, supported by many studies, the absorption band at 1550–1600 cm^{-1} is claimed to be uniquely indicative of the presence of C=N bonds [28, 29]. This result strongly agrees with the chemical composition of the polybenzoxazine having nitrogen incorporated into a Mannich bridge within its structure. Hemvichian *et al.* [15] identified the thermal decomposition products of aromatic amine based polybenzoxazines through TGA and GC-MS techniques. They found that the Mannich base compound is one of the generated products, which carry recombination and rearrangement abilities to form nitrogen containing char during the decomposition reaction. As validated by the study of Liu *et al.* [30], they found several possible bonding configurations of nitrogen atom in the carbon ring, as shown in Figure 4.7. In our case, the higher intensity of the absorption bands in the range from 1000 to 1600 cm^{-1} of the residual

char derived from the polybenzoxazine aerogel at sintering temperatures higher than 600 °C is strongly consistent with the evolution of secondary reaction products during the aerogel decomposition process, indicated by GC-TOF-MS analysis, as discussed later. Figure 4.8 shows the TGA and DTG thermograms of the bulk polybenzoxazine and the polybenzoxazine aerogel at different heating rates (10, 15, and 20 °C/min) under nitrogen atmosphere. Although, TGA curves of both the bulk and the aerogel reveal approximately similar decomposition behavior with a single distinct decomposition region, their characteristic details are very different. According to Figure 4.8a, the bulk polybenzoxazine begins to decompose at 240 °C. The degradation temperature at 10%weight loss falls between 336–349 °C and the highest mass loss rate is observed in the temperature range of 300–500 °C, corresponding to the production of a large amount of volatile material during the thermal decomposition process. Moreover, the bulk char yield at 800 °C lies between 26–27 wt%, as shown in the inset figure. This degradation behavior is in line with many other related works [21, 31]. Utilizing the Peak fit software, the DTG thermograms of the bulk polybenzoxazine at any heating rate could be divided into three individual components. The peak of each individual reaction shifts to higher temperature, when the heating rate is increased. All decomposition information derived at each heating rate from the Peak fit software is summarized in Table 4.1. Figure 4.8b shows the thermograms of the polybenzoxazine aerogel at various heating rates. Interestingly, the aerogel shows unusual thermal stability, as compared with the corresponding bulk polybenzoxazine. In addition to higher thermal stability it exhibits much higher char yield than the bulk at all heating rates. The degradation temperature at 10 %weight loss and the char yield at 800 °C of the polybenzoxazine aerogel fall between 416–425 °C and 49–53 wt%, respectively. Its decomposition process can be split into four components. All decomposition information derived from the aerogel is also tabulated in the Table 4.1. In the thermal decomposition process of various types of polybenzoxazines, two main chemical mechanisms are inevitably involved, viz. chain scission and dehydrogenation of the decomposition products [15, 16]. As reported in many publications, the primary decomposition products of bisphenol-A/aniline based polybenzoxazine are a combination of benzene derivatives, amines, phenolic compounds, Schiff base compounds, and

Mannich base compounds, During the decomposition process, these primary compounds can further react with each other to form secondary compounds, e.g. benzofuran derivatives, isoquinoline derivatives, biphenyl compounds, leading to the formation of a char with less reactivity [14-17, 24, 32].

From the results derived from GC-TOF-MS analysis, the percentages of the products evolved during the entire thermal decomposition process of the bulk benzoxazine and polybenzoxazine aerogel at a heating rate of 15 °C/min are tabulated in Table 4.2. The results are in support of the TGA results, in which the generated products from the polybenzoxazine aerogel decomposition contain more secondary compounds and other heterocyclic compounds than those generated from the bulk. These compounds can further react to form a very stable char. Thus, these MS results strongly confirm the greater amount of char yield generated by the polybenzoxazine aerogel, as compared to the bulk. The presence of the higher amount of the secondary and the heterocyclic compounds from the polybenzoxazine aerogel is a result of its contiguous microporous structure. The primary products which decompose within the structure have a longer retention time within the structure, resulting in higher opportunity for secondary reaction to form the secondary and heterocyclic compounds. As mentioned earlier, the MS result also confirms the high intensity of the organic FTIR absorption bands, indicating e chemical bonding between carbon and nitrogen of the residual char derived from the polybenzoxazine aerogel. As seen in Table 4.2, aniline and amine compounds are the main decomposition products of both types of the polybenzoxazine. The lower relative amount of aniline and amine compounds evolved during the decomposition process of the polybenzoxazine aerogel is consistent with a greater development of the secondary reaction, introducing the secondary decomposition products, i.e. benzofuran, benzoxazole, pyridine, and tetrazine. These decomposition products may then further form the residual char with carbon-nitrogen bonding via dehydrogenation reaction [15, 16].

Additionally, a most interesting property can be noticed from the TGA thermograms of both the bulk polybenzoxazine and the polybenzoxazine aerogel in Figure 4.8. Their residual char yields after carbonization systematically decrease when the heating rate is increased. There are several studies of the effect of heating

rate on the char yield in the decomposition reaction. They report a very parallel result that decomposition at a high heating rate provides high yields of volatile products. On the other hand, higher residual char yields are obtained from decomposition at a lower heating rate [33-36]. The study of Acma *et al.* [33], focused on the effect of the pyrolysis heating rate on the pyrolysis yield. They found that at a low heating rate, a high yield of solid char was obtained. Due to a slow rise in temperature, the decomposition products have a longer residence time to form secondary reactions, e.g. repolymerization and recondensation, directly affecting the increment of the resulting solid char. In contrast, at high heating rate, compounds with relatively low molecular weight were preferably formed via cracking reaction because the resistances to mass or heat transfer into the complex matrix are overcome, allowing a vigorous decomposition process to take place. In addition, comparing Figure 4.8a and 8b, variation of char yield at different heating rates is more prominently observed in the polybenzoxazine aerogel. As deduced from these results, due to the contribution of numerous micropores within the polybenzoxazine aerogel structure, the enhancement of char yield with decreasing heating rate is much more significant. This evidence implies that the porous structure of the polybenzoxazine aerogel acts as a synergistic factor, generating an enhancement of the residence time of the primary decomposition products, and leading to a prominent variation of the char yield with the heating rate.

From Figure 4.8, the peaks of the DTG thermograms are shifted to higher temperature when the heating rate is increased. As proposed by Kissenger [18], the activation energy of a thermally-activated process can be calculated from the shift of the inflection point in the TGA curves (i.e. the position in the peak of the DTG curves) at different heating rates. By employing the Kissenger model in Eq. 1 and the location of each individual peak from Table 4.1, the activation energy of each decomposition step can be calculated from the slope of a plot of $\ln (\beta/T_p^2)$ versus $1/T_p$, as shown in Figure 4.9, which presents Kissenger plots of each individual decomposition reaction for both the bulk polybenzoxazine and the polybenzoxazine aerogel, respectively. The resulting values of E_a are summarized in Table 4.1, As seen in the graphs, the relationship between $\ln (\beta/T_p^2)$ and $1/T_p$ of both samples

exhibits straight lines with high R^2 values for all decomposition steps, indicating excellent applicability of the Kissinger method. For the bulk polybenzoxazine, the obtained activation energies of stages 1, 2, and 3 are 109, 130, and 221 kJ/mol, respectively. These values are in agreement with the study of Tiptipakorn *et al.* [17]. Using the same calculation method, activation energies corresponding to the four decomposition steps of the polybenzoxazine aerogel were 90, 218, 362, and 464 kJ/mol, orderly. The difference in the activation energy of each individual decomposition step suggests that the bulk polybenzoxazine and the polybenzoxazine aerogel exhibit completely different decomposition mechanisms. As deduced from the area under each individual peak in Figure 4.8, the second steps of the thermal decomposition processes of both the bulk polybenzoxazine and the polybenzoxazine aerogel are the dominant steps. For each material, the activation energies of successive steps increase sequentially. Except for the first step which is discussed later, the latter three decomposition steps of the polybenzoxazine aerogel exhibit higher activation energies than the latter two steps of the bulk material, and the peaks corresponding to the maximum weight loss rate of these three decomposition steps are shifted to much higher temperatures, especially the last two steps. This implies that, the polybenzoxazine aerogel required higher energy for its thermal decomposition, as compared with the bulk. Moreover, this evidence also reveals that the polybenzoxazine aerogel exhibits superior degradation resistance and greater mass loss retardation than the bulk polybenzoxazine. This result strongly coincides with the TGA results, in which the polybenzoxazine aerogel shows much higher degradation temperature at 10% weight loss and greater char yield at any heating rate. As deduced from our previous investigations, the microporous network within the aerogel structure has a very strong influence on the decomposition process, which contributes to the enhancement of the secondary decomposition reactions. These reactions were reported to delay the mass loss rate during the thermal decomposition process. This kinetic investigation agrees well with the chemical structures of evolved gases during the decomposition process, as discussed later. The thermal decomposition mechanisms of various types of polybenzoxazines have been studied by many research groups [14-17, 24, 32]. Those studies can be summarized that the resulting decomposition products are a gaseous mixture, containing many species of

chemical compounds, e.g. benzene derivatives, amines, phenolic compounds, Mannich base compounds, Schiff base compounds, benzofuran derivatives, iso-quinoline derivatives, biphenyl compounds, and phenanthridine derivatives. To obtain more information about the reaction sequence and the corresponding products, the TG–FTIR technique, using a continuous real time analysis, was also applied in this work. However, since the thermal decomposition products were a gaseous mixture, the resolution of each individual chemical compound was slightly compromised.

Figure 4.10 shows the FTIR spectra of evolved gases during the thermal decomposition of both samples. These spectra were collected at the position corresponding to the peak of each decomposition process. The interpretation of these FTIR results can be described in terms of the following absorption bands. The sharp peak at 1280–1290cm^{-1} corresponds to the C-N stretching of aromatic amine. With support from the gas phase FTIR spectra of Schiff base compounds, the band at 1600 cm^{-1} is attributed to the presence of C=N in the compounds. The peak at 750 cm^{-1} is rassigned to vapor phase NH_2 wagging. These absorption peaks identify the amine compounds present [32, 37]. The prominent characteristics of phenolic compounds are absorption bands at 3650 and 1190 cm^{-1}, which are due to the free OH group and the C–O bond of phenol or substituted phenol, respectively [14]. From all spectra in Figure 4.10, we can clearly conclude that the decomposition products of both samples are principally composed of amine and phenolic compound. Due to the weakness of the characteristic signals of phenolic compounds, the spectra from the first decomposition step of the aerogel indicates that amine and Schiff base compounds are the major degradation components. On the other hand, the first decomposition step of the bulk polybenzoxazine presents relatively higher content of phenolic compounds, implied by the relatively greater intensity of the phenolic compound signatures at absorption bands of 3650 and 1190 cm^{-1}. This outcome is in accordance with both the activation energy and the chemical structure of the bulk polybenzoxazine and the polybenzoxazine aerogel. As mentioned earlier, a small amount of Schiff bases are formed as defect structures or terminal groups during the polybenzoxazine aerogel synthesis. Thus, to evolve amine or Schiff base compounds during the thermal decomposition process, only one carbon-carbon single bond must

be ruptured for the aerogel, whereas, two single bonds have to be broken in the Mannich bridge of the bulk polybenzoxazine. This interpretation provides a rationale for the more dominant signal of the amine and the Schiff base compounds evolved within the first decomposition step of the polybenzoxazine aerogel. This analysis is also consistent with the activation energies of the first decomposition steps, in which the polybenzoxazine aerogel exhibits a slightly lower activation energy and decomposition temperature than the bulk.

Moreover, as additional support for our interpretation of the ability of the microporous morphology to enhance the thermal stability of polybenzoxazine aerogel, a different type of bulk polybenzoxazine and its corresponding aerogel were synthesized, and their thermal stabilities were also investigated. Figure 4.11 shows TG and DTG thermograms of the bisphenol-A/ tetraethylenepentamine (TEPA) based bulk polybenzoxazine and its corresponding aerogel under nitrogen atmosphere at a heating of 15 °C/min. As expected, this polybenzoxazine aerogel also exhibits a much higher degradation temperature and char yield than the bulk. The decomposition temperature at 10%weight loss and the char yield at 800 °C of the bisphenol-A/TEPA based polybenzoxazine aerogel increased by 12% and 174%, respectively, over those of the bulk.

4.5 Conclusions

In this study, the improvement in thermal stability of the bisphenol-A/aniline based polybenzoxazine aerogel comparing with that of the corresponding bulk polybenzoxazine was investigated in the temperature range up to 900 °C by measuring degradation temperature, weight loss, chemical compositions of evolved gas and residual char, and the relative amount of each chemical compound in the evolved gases. The activation energy of each decomposition step was also determined using the Kissinger method. All evidence in this study indicates that the difference in thermal degradation stability is the result of the dissimilar morphology which appears to have a considerable effect on the degradation temperature, char yield, and char property. The decomposition temperature and the char yield of the bisphenol-A/aniline based polybenzoxazine aerogel increase up to 24% and 97%

higher than those of the bulk, respectively. The contiguous micropores within the polybenzoxazine aerogel structure introduce an enhancement of the residence time of the primary decomposition products, which thus have greater opportunity to form secondary reactions. Furthermore, influenced by their different structures, the bulk polybenzoxazine and the polybenzoxazine aerogel exhibit significantly different decomposition mechanisms, as seen from their activation energies and maximum mass loss rates of each individual decomposition step. In addition, the residual char yields derived from both the bulk polybenzoxazine and the polybenzoxazine aerogel are increased with decrease in the heating rate. The porous structure of the polybenzoxazine aerogel is proved to be a synergetic factor for an enhancement of the char yield value in the TGA experiment.

4.6 Acknowledgements

This research is financially supported by the Thailand Research Fund (TRF), the National Center of Excellence for Petroleum, Petrochemicals, and Advanced Materials, and the Ratchadapisake Sompote Fund, Chulalongkorn University. Additionally, the authors would like to thank Mr. Sunan Tiptipakorn for his kind kinetics advice, as well as Mr. Uthen Thubsuang and Miss Sirat Ratanadilok Na Phuket for facilitating the work.

4.7 References

1. Lorjai, P., Chaisuwan, T., and Wongkasemjit, S. (2009) Porous structure of polybenzoxazine-based organic aerogel prepared by sol–gel process and their carbon aerogels. Journal of Sol-Gel Science and Technology, 52, 56-64.
2. Horikawa, T, Hayashi, J., and Muroyama, K. (2004) Size control and characterization of spherical carbon aerogel particles from resorcinol–formaldehyde resin. Carbon, 42, 169-175.

3. Liu, N., Zhang, S., Fu, R., Dresselhaus, M.S., Dresselhaus G. (2006) Carbon aerogel spheres prepared via alcohol supercritical drying. Carbon, 44, 2430-2436.

4. Wu, D. and Fu, R. (2005) Fabrication and Physical Properties of Organic and Carbon Aerogel Derived from Phenol and Furfural. Journal of Porous Materials, 12, 311-316.

5. Biesmans, G., Mertens, A., Duffours, L., Woignier, T., and Phalippou, J. (1998) Polyurethane based organic aerogels and their transformation into carbon aerogels. Journal of Non-Crystalline Solids, 225, 64-68.

6. Stańczyk, K. and Kisielow, W. (1994) Influence of hydropyrolysis parameters on char yield, properties and combustion reactivity. Fuel, 73, 660-665.

7. Kumar, M., Gupta, R.C., and Sharma, T. (1992) Effects of carbonization conditions on the yield and chemical composition of Acacia and Eucalyptus wood chars. Biomass Bioenergy, 3, 411-417.

8. Ishida, H. and Sanders, D.P. (2000) Regioselectivity and Network Structure of Difunctional Alkyl-Substituted Aromatic Amine-Based Polybenzoxazines. Macromolecules, 33, 8149-8157.

9. Kimura, H., Taguchi, S., and Matsumoto, A. (2001) Studies on New Type of Phenolic Resin Curing Reaction of Bisphenol A-Based Benzoxazine with Bisoxazoline and the Properties of the Cured Resin. II. Cure Reactivity of Benzoxazine. Journal of Applied Polymer Science, 79, 2331-2339.

10. Ishida, H. and Ohba, S. (2005) Synthesis and characterization of maleimide and norbornene functionalized benzoxazines. Polymer, 46, 5588-5595.

11. Ning, X. and Ishida, H. (1994) Phenolic materials via ring-opening polymerization: Synthesis and characterization of bisphenol-A based benzoxazines and their polymers. Journal of Polymer Science Part A: Polymer Chemistry, 32, 1121-1129.

12. Ning, X. and Ishida, H. (1994) Phenolic materials via ring-opening polymerization of benzoxazines: Effect of molecular structure on mechanical and dynamic mechanical properties. Journal of Polymer Science Part B: Polymer Physics, 32, 921-927.

13. Ishida, H. and Allen, D. (1996) Mechanical characterization of copolymers based on benzoxazine and epoxy. Polymer, 37, 4487-4495.

14. Low, H.Y. and Ishida, H. (1999) Structural effects of phenols on the thermal and thermo-oxidative degradation of polybenzoxazines. Polymer, 40, 4365-4376.

15. Hemvichian, K. and Ishida, H. (2002) Thermal decomposition processes in aromatic amine-based polybenzoxazines investigated by TGA and GC–MS. Polymer, 43, 4391-4402.

16. Hemvichian, K., Kim, H.D., and Ishida, H. (2005) Identification of volatile products and determination of thermal degradation mechanisms of polybenzoxazine model oligomers by GC-MS. Polymer Degradation and Stability, 87, 213-224.

17. Tiptipakorn, S., Damrongsakkul, S., Ando, S., Hemvichian, K., and Rimdusit, S. (2007) Thermal degradation behaviors of polybenzoxazine and silicon-containing polyimide blends. Polymer Degradation and Stability, 92, 1265-1278.

18. Kissinger, H.E. (1957) Reaction kinetics in differential thermal analysis. Analytical Chemistry, 29, 1702-1706.

19. Chen, Y. and Wang, Q. (2007) Thermal oxidative degradation kinetics of flame-retarded polypropylene with intumescent flame-retardant master batches in situ prepared in twin-screw extruder. Polymer Degradation and Stability, 92, 280-291.

20. Ishida, H. (1996) US Patent 5 543 516.

21. Agag, T. and Takeichi, T. (2003) Synthesis and Characterization of Novel Benzoxazine Monomers Containing Allyl Groups and Their High Performance Thermosets. Macromolecule, 36, 6010-6017.

22. Takeichi, T., Guo, Y., and Rimdusit, R. (2005) Performance improvement of polybenzoxazine by alloying with polyimide: effect of preparation method on the properties. Polymer, 46, 4909-4916.

23. Su, Y.C., Chen, W.C., and Chang, F.C. (2004) Investigation of the Thermal Properties of Novel Adamantane-Modified Polybenzoxazine. Journal of Applied Polymer Science, 94, 932-940.

24. Hemvichian, K., Laobuthee, A., Chirachanchai, S., and Ishida, H. (2002) Thermal decomposition processes in polybenzoxazine model dimers investigated by TGA–FTIR and GC–MS. Polymer Degradation and Stability, 76, 1-15.

25. Ishida, H. and Krus, C.M. (1998) Synthesis and Characterization of Structurally Uniform Model Oligomers of Polybenzoxazine. Macromolecules, 31, 2409-2418.

26. Istková, M.K., Filip, P., Weiss, Z.K., and Peter, R. (2004) Influence of metals on the phenol–formaldehyde resin degradation in friction composites. Polymer Degradation and Stability, 84, 49-60.

27. Khawwam, A.A., Jama, C., Goudmand, P., Dessaux, O., Achari, A.E., Dhamelincourt, P., and Patrat, G. (2002) Characterization of carbon nitride layers deposited by IR laser ablation of graphite target in a remote nitrogen plasma atmosphere: nanoparticle evidence. Thin Solid Films, 408, 15-25.

28. Li, C., Yang, X., Yang, B., Yan, Y., and Qian, Y. (2007) Synthesis and characterization of nitrogen-rich graphitic carbon nitride. Materials Chemistry and Physics, 103, 427-432.

29. Ong, C.W., Zhao, X.A., Tsang, Y.C., Choy, C.L., and Chan, P.W. (1996) Effects of substrate temperature on the structure and properties of reactive pulsed laser deposited CNx films. Thin Solid Films, 280, 1-4.

30. Liu, Y., Jiaa, C., and Do, H. (1999) Correlation of deposition and IR properties of amorphous carbon nitride films. Surface and Coatings Technology, 115, 95-102.

31. Wang, Y.X. and Ishida, H., (2002) Development of low-viscosity benzoxazine resins and their polymers. Journal of Applied Polymer Science, 86, 2953-2966.

32. Low, H.Y. and Ishida, H. (1998) Mechanistic study on the thermal decomposition of polybenzoxazines: Effects of aliphatic amines. Journal of Polymer Science Part B: Polymer Physics, 36, 1935-1946.

33. Acma, H.H., Yaman, S., and Kucukbayrak, S. (2006) Effect of heating rate on the pyrolysis yields of rapeseed. Renew Energy, 31, 803-810.

34. Yaman, S. (2004) Pyrolysis of biomass to produce fuels and chemical feedstocks. Energy Conversion and Management, 45, 651-671.

35. Sharma, R.K. and Hajaligol, M.R. (2003) Effect of pyrolysis conditions on the formation of polycyclic aromatic hydrocarbons (PAHs) from polyphenolic compounds. Journal of Analytical and Applied Pyrolysis, 66, 123-144.

36. Watanabe, M., Aizawa, Y., Iida, T., Levy, C., Aida, T.M., and Inomata, H. (2005) Glucose reactions within the heating period and the effect of heating rate on the reactions in hot compressed water. Carbohydrate Research, 340, 1931-1939.

37. Arasi, A.Y., Jeyakumari, J.J.L., Sundaresan, B., Dhanalakshmi, V., and Anbarasan, R. (2009) The structural properties of Poly(aniline)-Analysis via FTIR spectroscopy. Spectrochimica Acta Part A: Molecular and Biomolecular Spectroscopy, 74, 1229-1234.

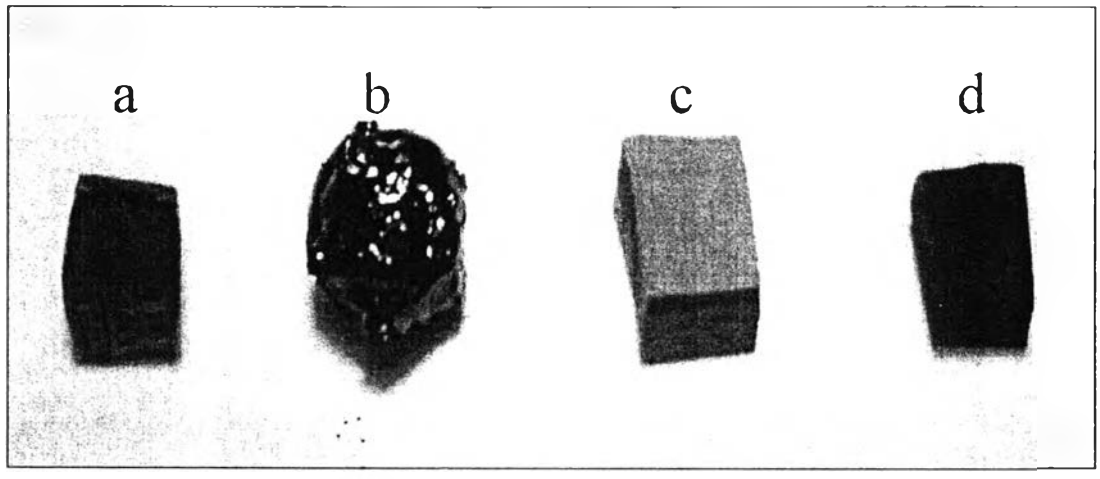

Figure 4.1 Photographs of (a) bulk polybenzoxazine, (b) residual char from bulk polybenzoxazine, (c) polybenzoxazine aerogel, and (d) residual char from polybenzoxazine aerogel. . .

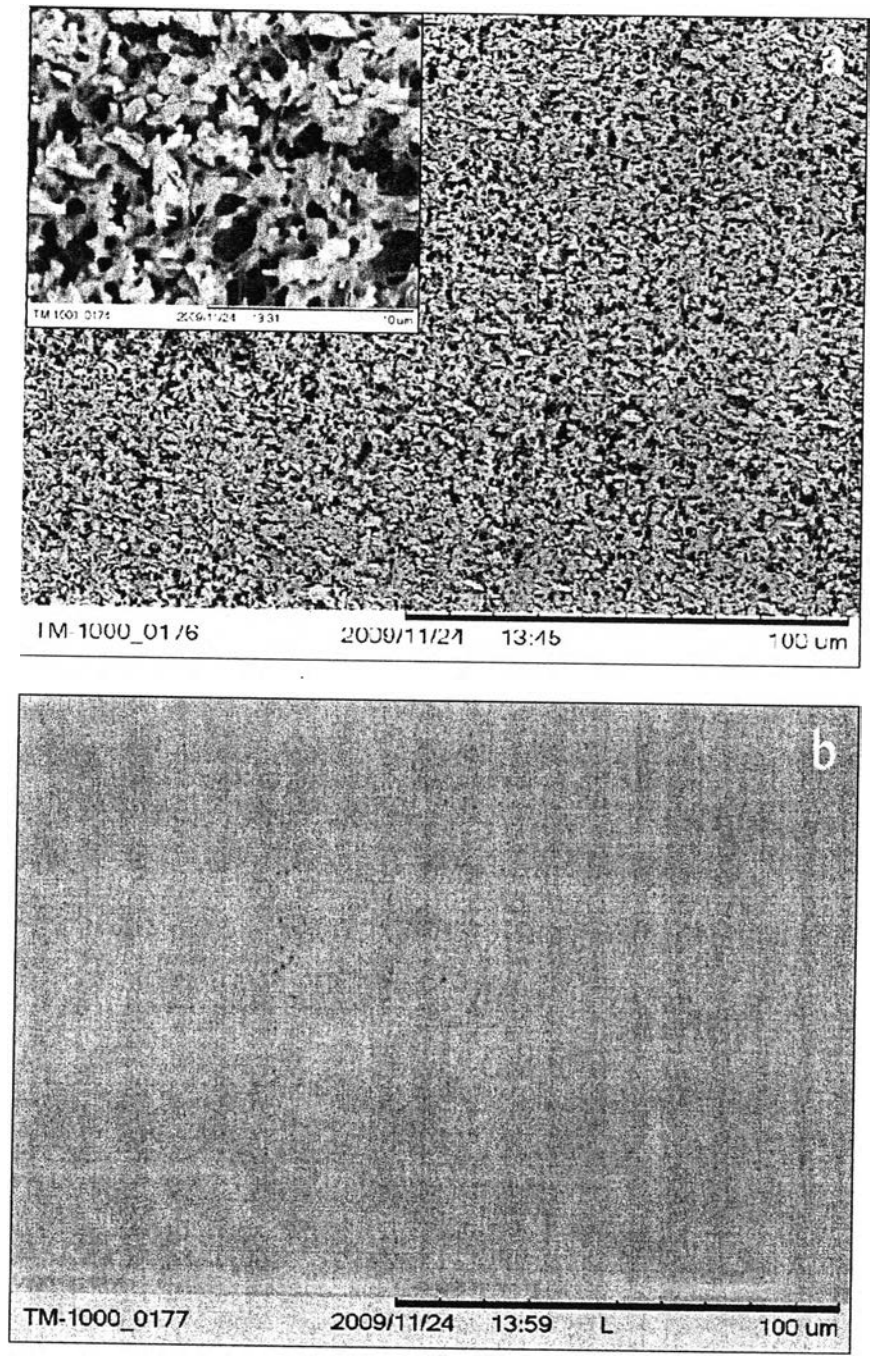

Figure 4.2 SEM micrographs of (a) polybenzoxazine aerogel and (b) bulk polybenzoxazine.

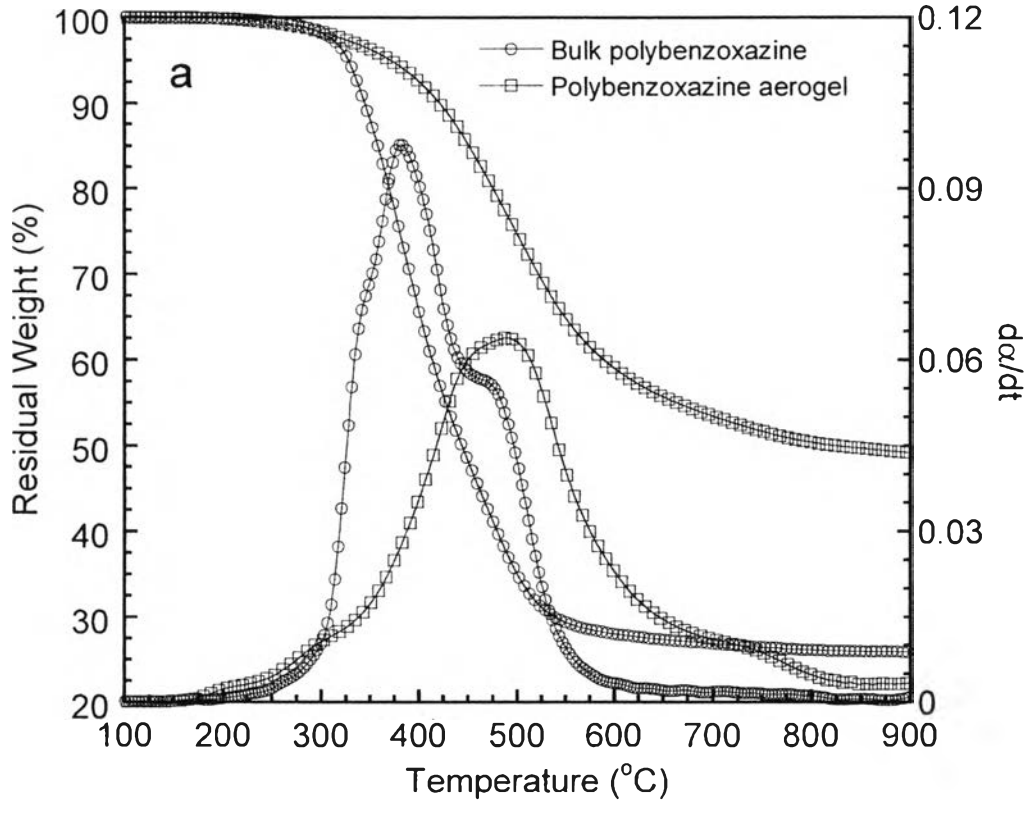

Figure 4.3 TGA and DTG thermograms of bulk polybenzoxazine and polybenzoxazine aerogel at a heating rate of 15°C/min.

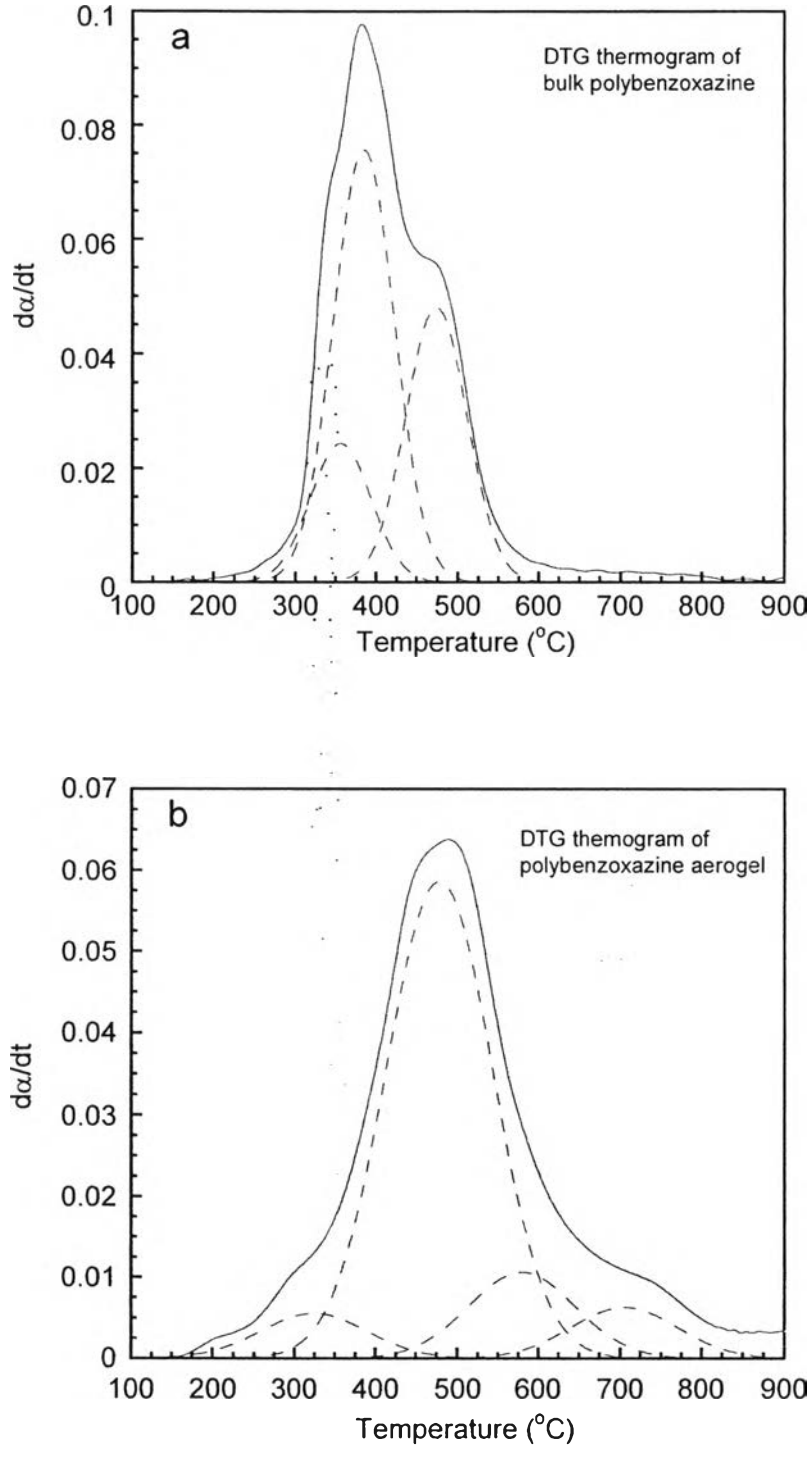

Figure 4.4 DTG curves and associated individual peaks of (a) bulk polybenzoxazine and (b) polybenzoxazine aerogel at a heating rate of 15°C/min.

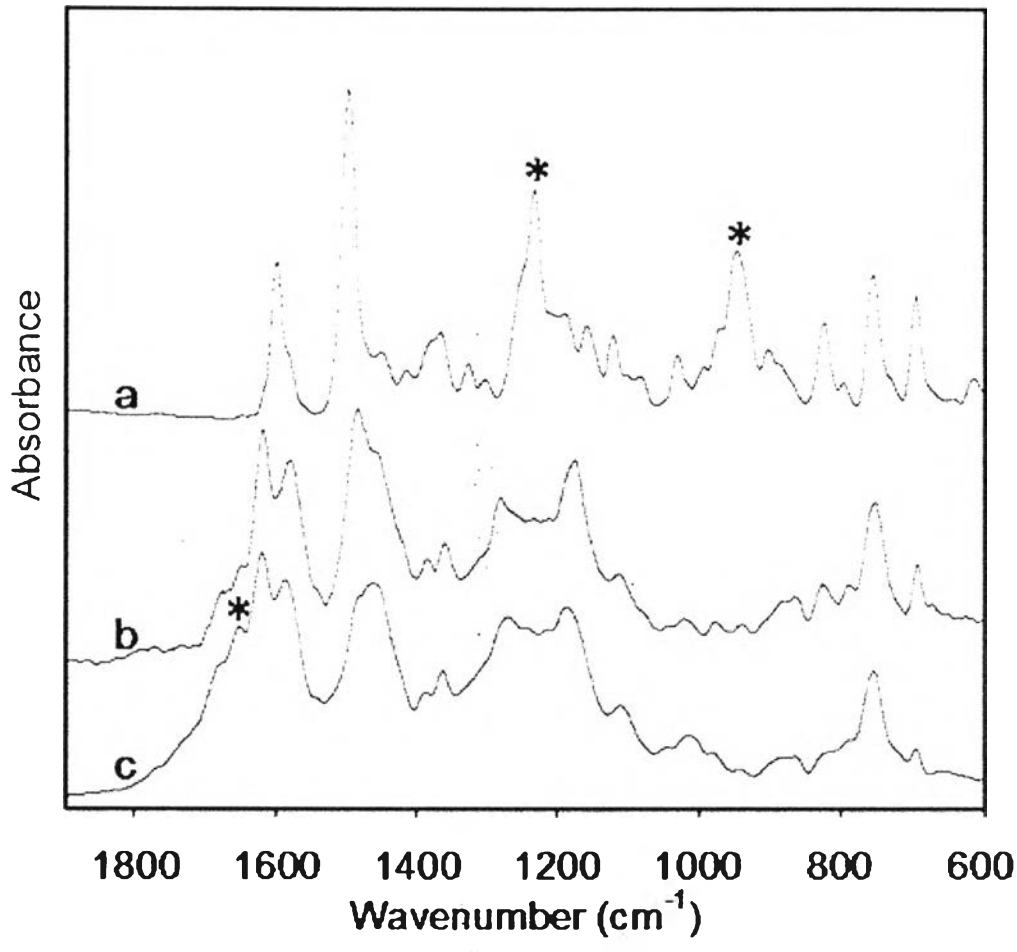

Figure 4.5 FTIR spectra of (a) benzoxazine monomer, (b) bulk polybenzoxazine, and (c) polybenzoxazine aerogel. The asterisks indicate peaks discussed in the text.

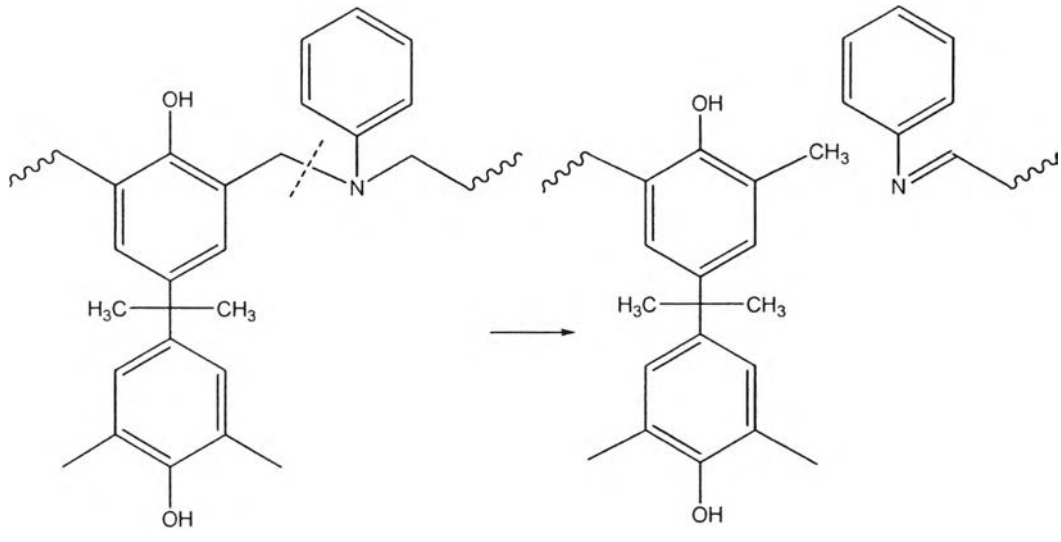

Scheme 4.1 Mechanism for Schiff base formation from chain cleavage at Mannich bridge within polybenzoxazine [14, 15, 24].

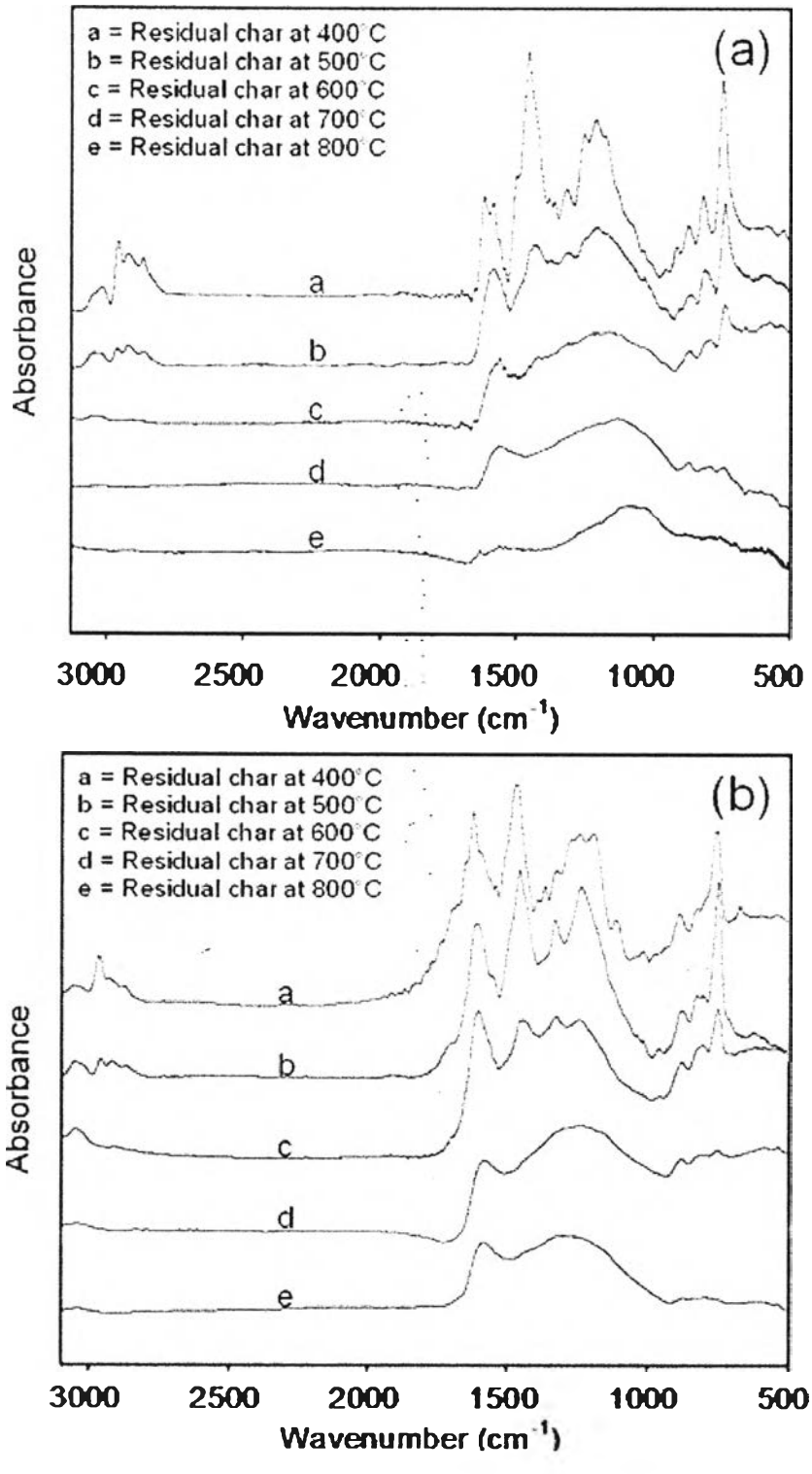

Figure 4.6 FTIR spectra of residual char derived from (a) bulk polybenzoxazine and (b) polybenzoxazine aerogel after carbonization at various temperatures at a heating rate of 15°C/min.

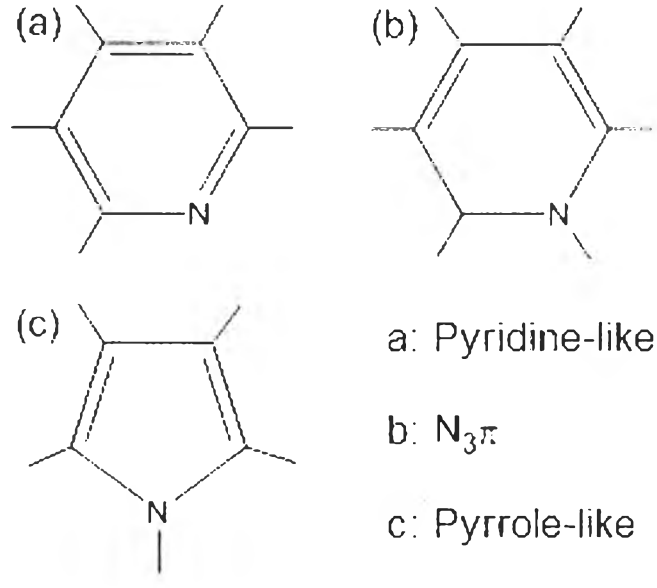

Figure 4.7 Possible bonding configurations of nitrogen atom in carbon ring [30].

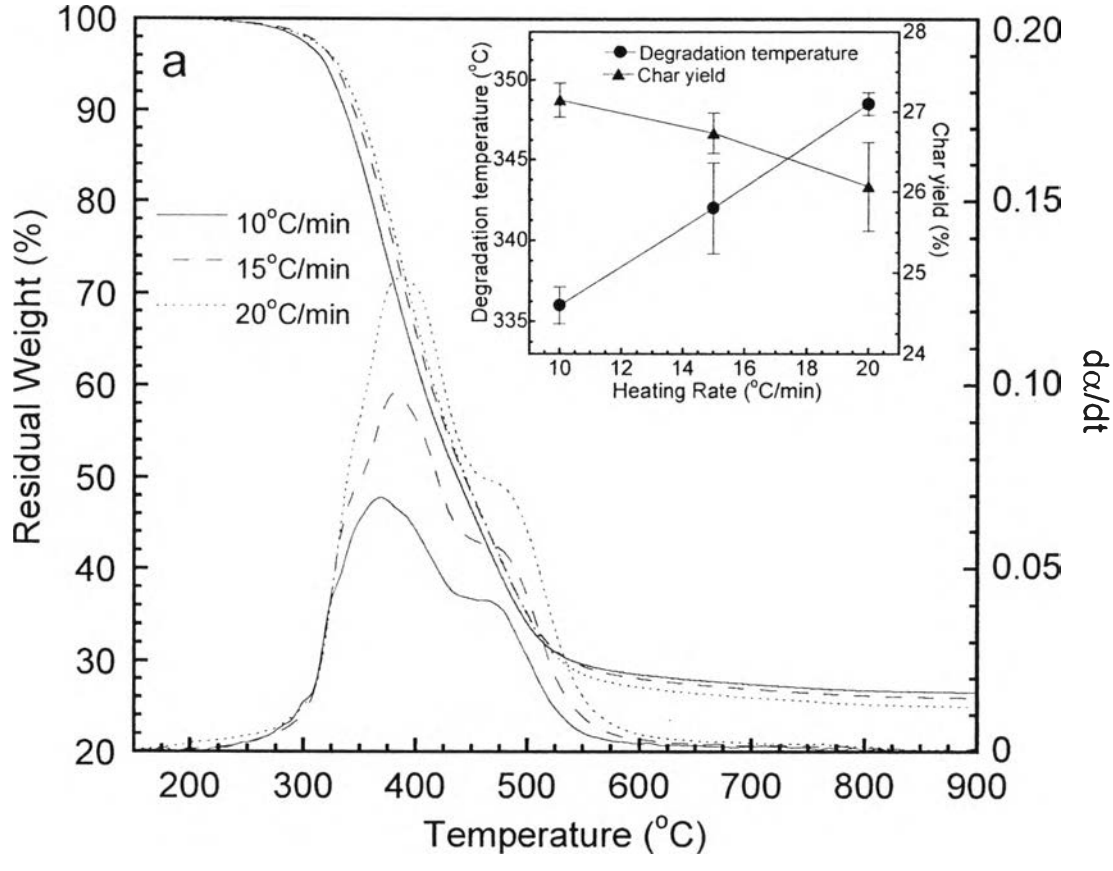
a
Residual Weight (%)
Temperature (°C)
dα/dt
10°C/min
15°C/min
20°C/min
Degradation temperature
Char yield
Degradation temperature (°C)
Char yield (%)
Heating Rate (°C/min)

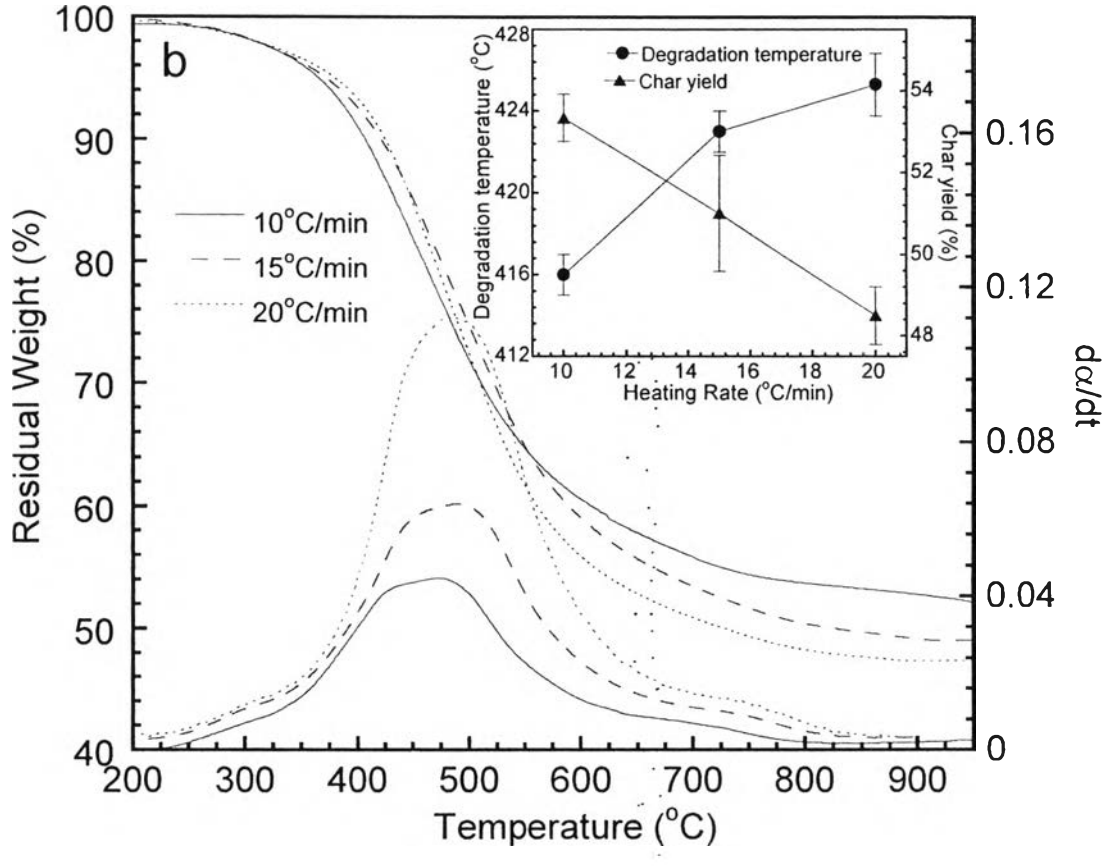

Figure 4.8 TGA and DTG analyses of (a) bulk polybenzoxazine, and (b) polybenzoxazine aerogel at different heating rates.

Table 4.1 Summary of characteristics of individual DTG peaks derived using Peak fit software and associated activation energies obtained using the Kissinger method for bulk polybenzoxazine and polybenzoxazine aerogel

Polybenzoxazine (bulk)	T_p (°C)			Area (%)			Ea (KJ/mol)
	Heating rate (β) (°C/min)			Heating rate (β) (°C/min)			
	10	15	20	10	15	20	
Stage 1	344 ± 1	353 ± 2	362 ± 2	15 ± 4	18 ± 4	23 ± 3	109
Stage 2	374 ± 2	385 ± 1	392 ± 1	50 ± 3	50 ± 4	45 ± 2	130
Stage 3	466 ± 2	475 ± 2	479 ± 2	35 ± 1	32 ± 1	32 ± 1	221
T_d (10%weight loss)	336 ± 2	342 ± 2	349 ± 1				
Char yield	27.1 ± 0.2	26.7 ± 0.3	26.1 ± 0.6				
Polybenzoxazine (Aerogel)							
Stage 1	311 ± 2	323 ± 1	332 ± 2	6 ± 3	7 ± 1	7 ± 1	90
Stage 2	469 ± 1	477 ± 1	483 ± 1	73 ± 2	72 ± 3	73 ± 1	218
Stage 3	574 ± 1	581 ± 2	585 ± 2	15 ± 1	15 ± 1	15 ± 1	362
Stage 4	699 ± 1	707 ± 2	710 ± 3	6 ± 2	6 ± 2	5 ± 1	464
T_d (10%weight loss)	416 ± 1	423 ± 1	425 ± 2				
Char yield	53.3 ± 0.6	51.0 ± 1.4	48.5 ± 0.7				

Table 4.2 Percentage of each decomposition product generated from the entire carbonization process of bulk polybenzoxazine and polybenzoxazine aerogel under nitrogen atmosphere

Polybenzoxazine (Bulk)			Polybenzoxazine (Aerogel)		
Mw	Name	Percentage	Mw	Name	Percentage
Primary decomposition products			Primary decomposition products		
93	Aniline	78.497	93	Aniline	64.217
107	Aminotoluene	7.081	94	Phenol	13.693
108	Phenol, 2-methyl	3.335	78	Benzene	7.866
122	Phenol, 2,3-dimethyl	0.791	107	Toluidine	3.595
94	Phenol	0.728	108	Phenol, 2-methyl	1.999
136	Phenol, 3-(1-methylethyl)	0.543	103	Benzonitrile	1.614
120	Benzene, 1-ethyl-2-methyl	0.541	108	Phenol, 4-methyl	0.791
120	Benzene, 1,2,3-trimethyl	0.533	92	Toluene	0.386
136	Aniline, N-methyl	0.480	122	Phenol, 2,3-dimethyl	0.321
150	Phenol, p-tret-butyl	0.465	117	Benzonitrile, 2-methyl	0.404
165	Mannich base compound	0.423	120	Benzene, 1,2,3-trimethyl	0.305
121	Benzenamine, 3,5-dimethyl	0.412	122	Phenol, 2,4-dimethyl	0.260
241	Mannich base compound	0.358	122	Phenol, 4-ethyl	0.233
108	Phenol, 4-methyl	0.344	104	Styrene	0.192
122	Phenol, 4-ethyl	0.321	116	Benzene, 1-propynyl	0.177
122	Phenol, 2,4-dimethyl	0.252	120	Benzene, 1-ethyl-4-methyl	0.112
108	Phenol, 2-methyl	0.241	107	Aniline, N-methyl	0.112
122	Phenol, 2-ethyl	0.222	106	Xylene	0.094
199	Mannich base compound	0.219			
92	Toluene	0.188			
121	Dimethylbenzene	0.181			
136	Phonol, 2-ethyl -5-methyl	0.165			
106	Xylene	0.179			
134	p-Isoprophenylphenol	0.102			
Secondary decomposition products			Secondary decomposition products		
118	Benzofuran	0.585	118	Benzofuran	1.230
143	Isoquinoline, 1-methyl	0.154	119	Benzoxazole	0.887
			133	Benzoxazole, 2-methyl	0.239
			132	Benzofuran, 2-methyl	0.202
			117	5H-1-Pyridine	0.196
			82	1,2,4,5- Tetrazine	0.079

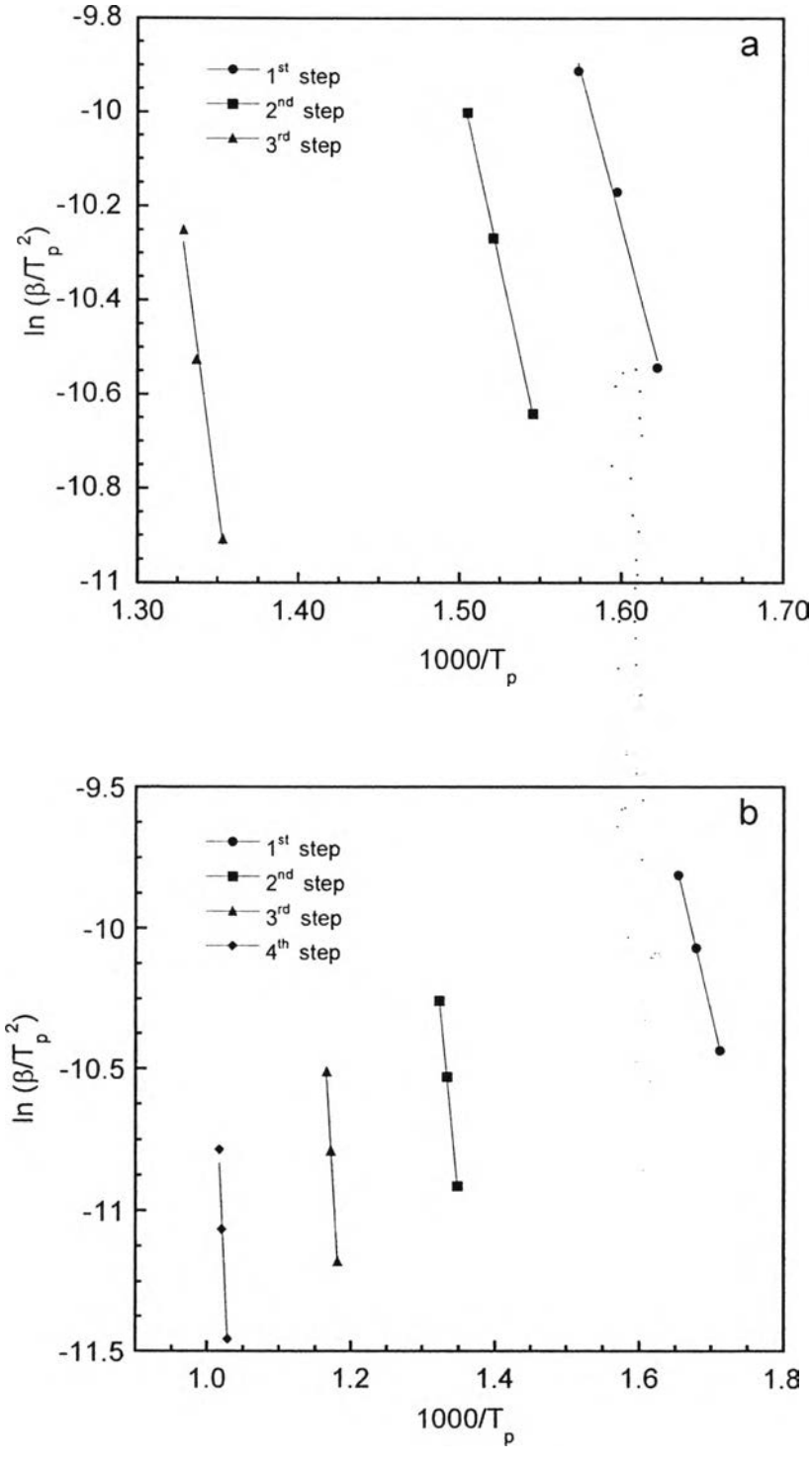

Figure 4.9 Plots of ln (β/T_p^2) versus $1/T_p$ for each decomposition step at different heating rates from DTG analysis via the Kissinger method for (a) bulk polybenzoxazine and (b) polybenzoxazine aerogel.

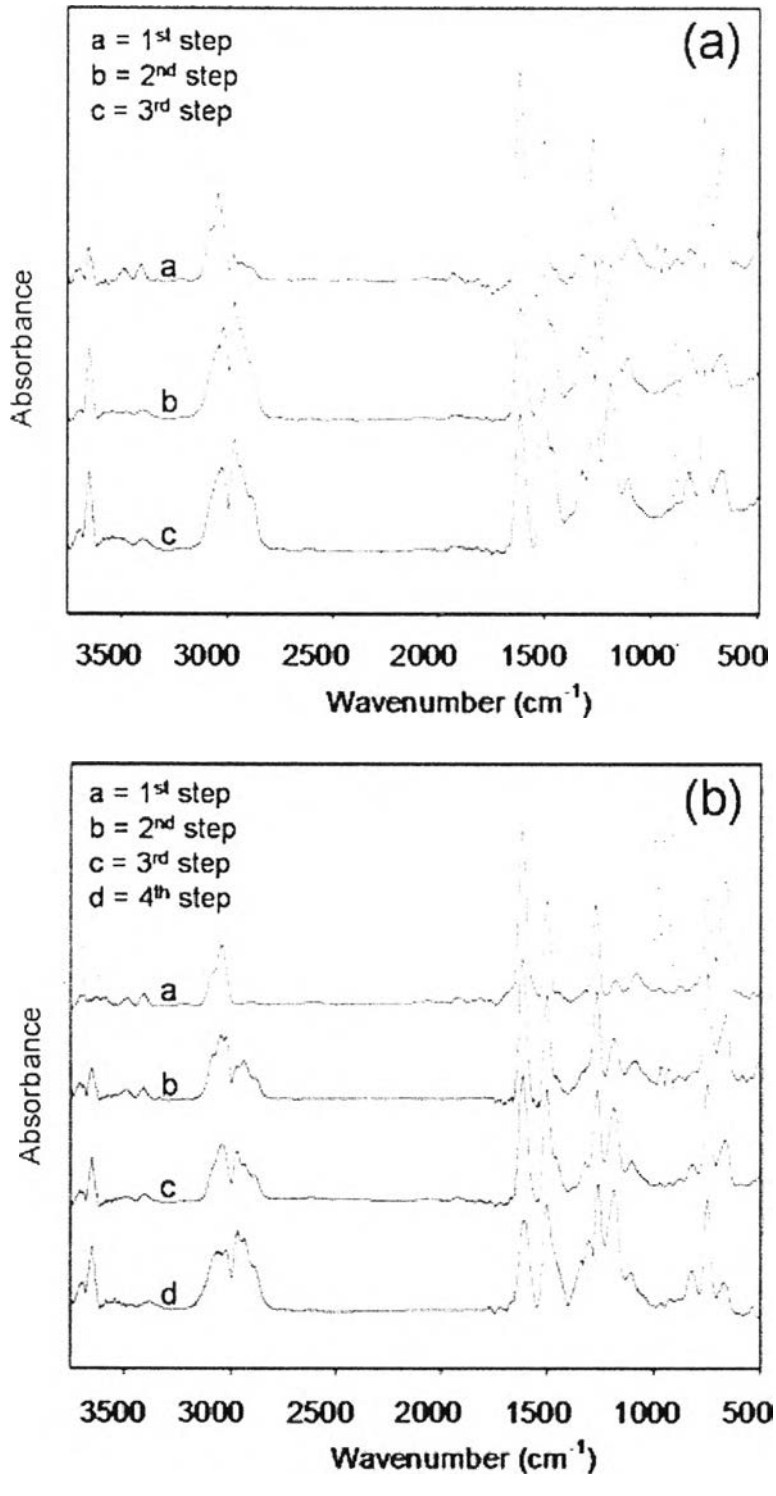

Figure 4.10 FTIR spectra of the decomposition products of (a) bulk polybenzoxazine, and (b) polybenzoxazine aerogel generated during each decomposition step at a heating rate of 15°C/min.

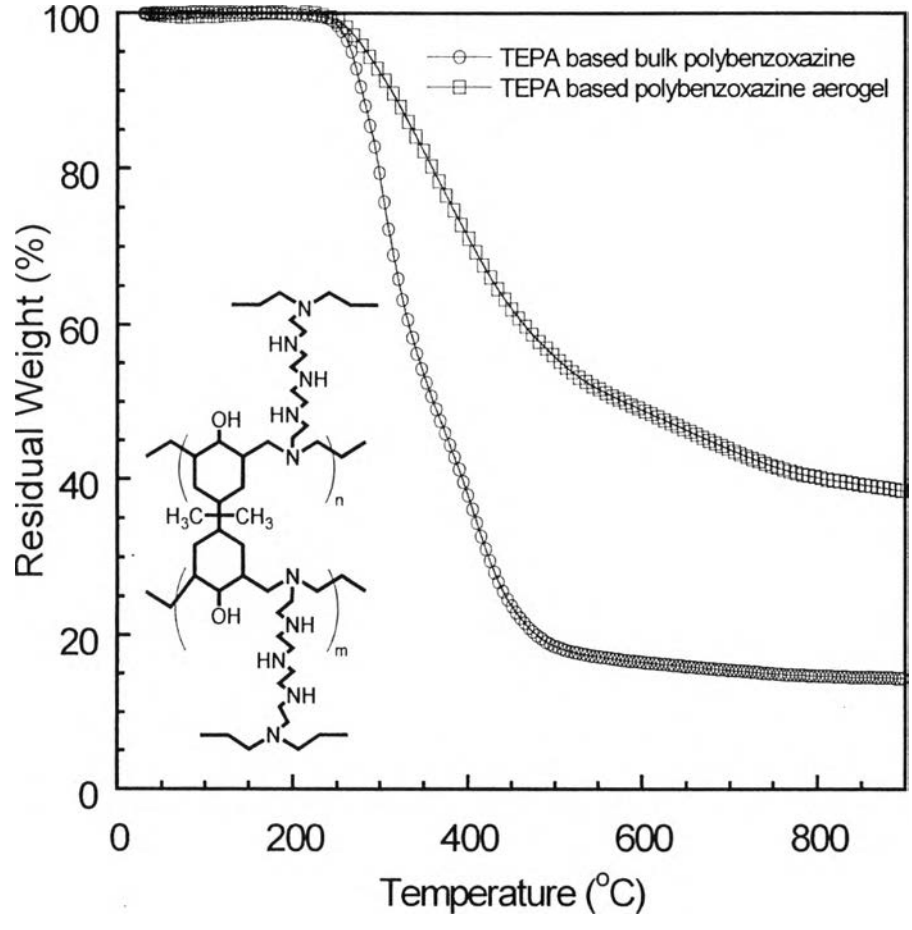

Figure 4.11 TGA and DTG analyses of bisphenol-A/tetraethylenepentamine (TEPA) based bulk polybenzoxazine and its corresponding aerogel under nitrogen atmosphere at a heating rate of 15°C/min.